Supporting Information

Nickle Induced Electronic Structure Regulation of Cobalt Hydroxide for Enhanced Water Oxidation

Yuan Wang,[a] Chenxi Yang,[b] Yunxia Huang,[a] Zhimin Li,[a,] Zuozhong Liang,[c,]* Guozhong Cao[d,]**

[a]School of Advanced Materials and Nanotechnology, Xidian University, Xi'an 710126, P.R. China

[b]Sinopec Beijing Research Institute of Chemical Industry, Beijing, 100013, P.R. China

[c]School of Chemistry and Chemical Engineering, Shaanxi Normal University, Xi'an 710119, P.R. China

[d]Department of Materials and Engineering, University of Washington, Seattle, Washington 98195-2120, United States

Corresponding authors: Zhimin Li E-mail: zmli@mail.xidian.edu.cn

Zuozhong Liang E-mail: liangzuozhong@snnu.edu.cn

Guozhong Cao E-mail: gzcao@u.washington.edu

Table S1. The refined unit cell parameters of $Co(OH)_2$ and $Ni_xCo_y(OH)_2$.

Sample	*a* (Å)	*b* (Å)	*c* (Å)	*Volume* (Å^3)
$Co(OH)_2$	9.42455	9.42455	8.96842	689.871
$Ni_{0.15}Co_{0.85}(OH)_2$	9.45787	9.45787	9.01376	698.270
$Ni_{0.25}Co_{0.75}(OH)_2$	9.39444	9.51605	9.01946	701.210
$Ni_{0.35}Co_{0.65}(OH)_2$	9.45429	9.52132	9.00069	703.297

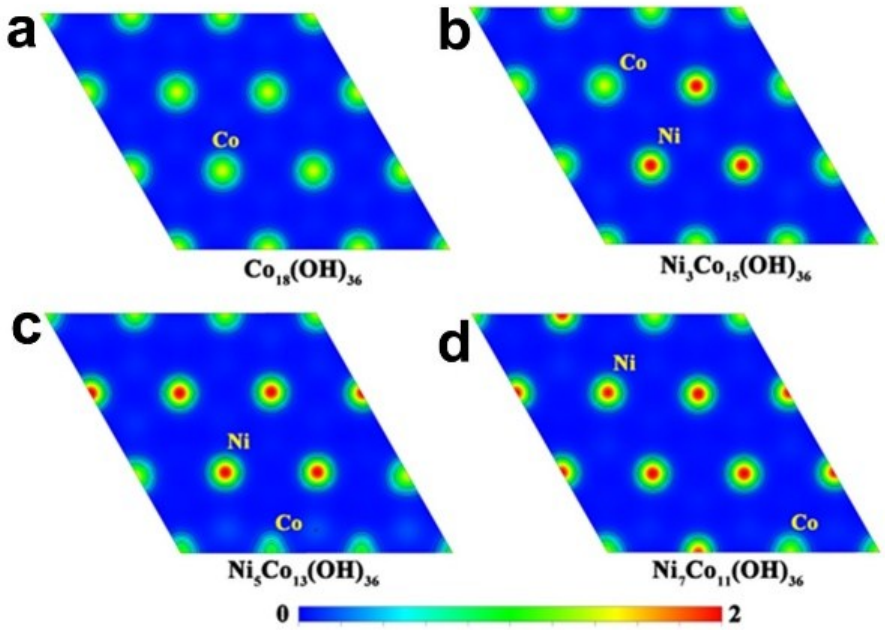

Fig. S1. Charge density distribution plots of (001) face for the bulk $Co(OH)_2$, and $Ni_xCo_y(OH)_2$ models.

Table S2. Bader charge of Co, Ni, O and H atoms in bulk $Co(OH)_2$, and $Ni_xCo_y(OH)_2$ models. All the data is expressed per atom

	Co	Ni	O	H	ΔO-H	ΔCo-O	ΔCo-O-H
$Co_{18}(OH)_{36}$	7.907	-	7.112	0.435	-	-	-
$Ni_3Co_{15}(OH)_{36}$	7.889	9.015	7.105	0.439	-0.001658	-0.024103	-0.019269
$Ni_5Co_{13}(OH)_{36}$	7.880	9.002	7.106	0.437	-0.003450	-0.0326543	-0.030374
$Ni_7Co_{11}(OH)_{36}$	7.880	8.965	7.108	0.436	-0.002878	-0.0310643	-0.029828

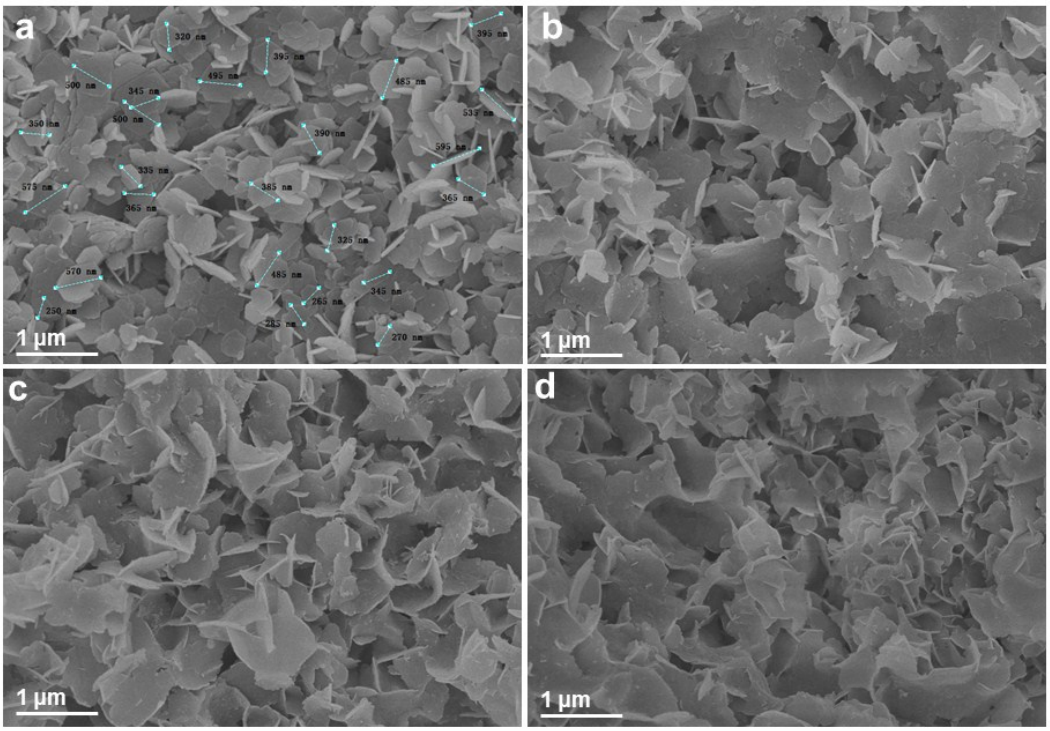

Fig. S2. SEM images of $Co(OH)_2$ (a), $Ni_{0.15}Co_{0.85}$-LDH (b), $Ni_{0.25}Co_{0.75}$-LDH (c), and $Ni_{0.35}Co_{0.65}$-LDH (d)

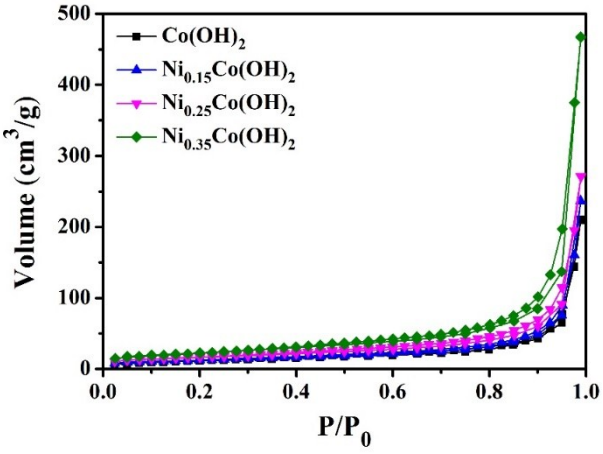

Fig. S3. Nitrogen adsorption/desorption isotherms of the $Co(OH)_2$ and Ni_xCo_y-LDH materials.

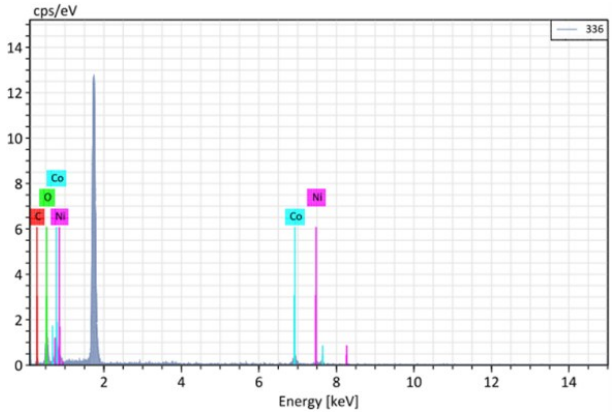

Fig. S4. The EDS pattern of the $Ni_{0.25}Co_{0.75}(OH)_2$.

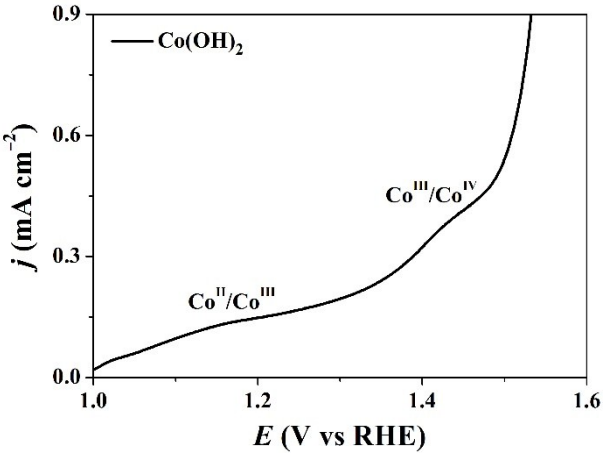

Fig. S5. The LSV curve of the $Co(OH)_2$

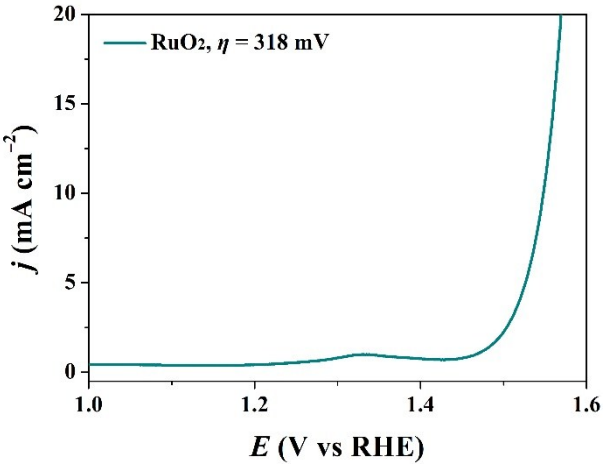

Fig. S6. The LSV curve of the RuO_2

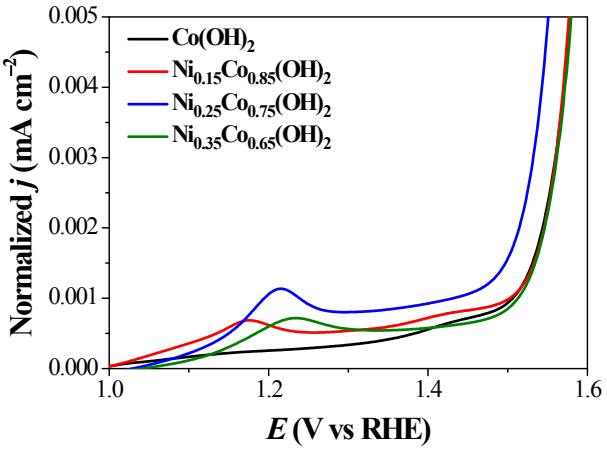

Fig. S7. The normalized LSV curves of the $Co(OH)_2$ and $Ni_xCo_y(OH)_2$ materials based on the BET surface area.

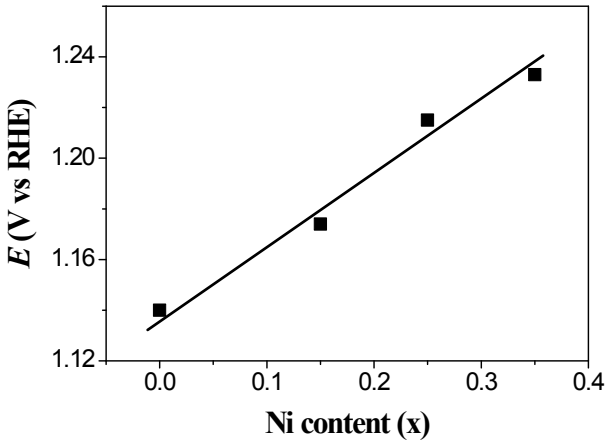

Fig. S8. The potential of $Co^{II/III}$ oxidation (*E*) versus the Ni content (x) for the $Co(OH)_2$ and $Ni_xCo_y(OH)_2$ materials

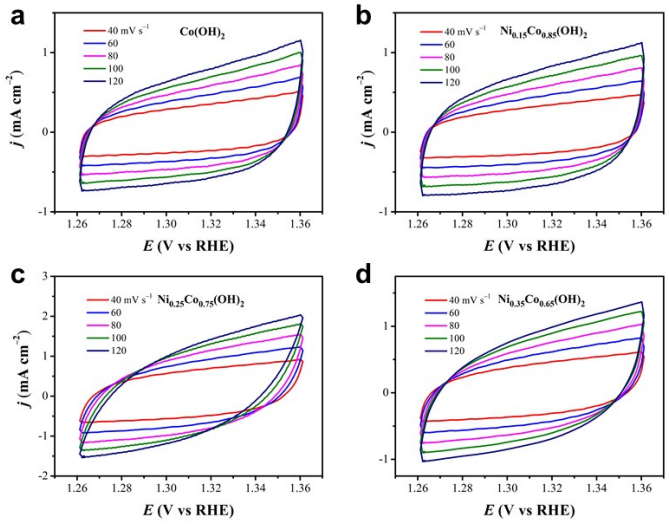

Fig. S9. CV curves of the $Co(OH)_2$ (a), $Ni_{0.15}Co_{0.85}(OH)_2$ (b), $Ni_{0.25}Co_{0.75}(OH)_2$ (c), and $Ni_{0.35}Co_{0.65}(OH)_2$ (d) measured with different scan rates.

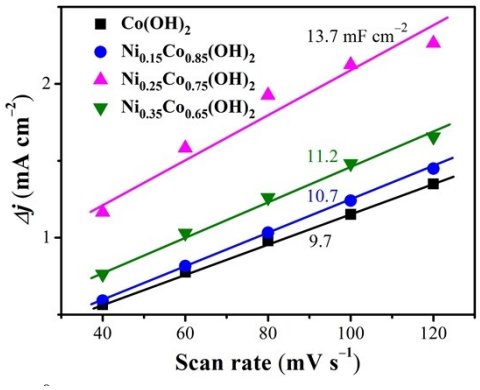

Fig. S10. Plots of the current density vs scan rate for the $Co(OH)_2$, $Ni_{0.15}Co_{0.85}(OH)_2$, $Ni_{0.25}Co_{0.75}(OH)_2$, and $Ni_{0.35}Co_{0.65}(OH)_2$.

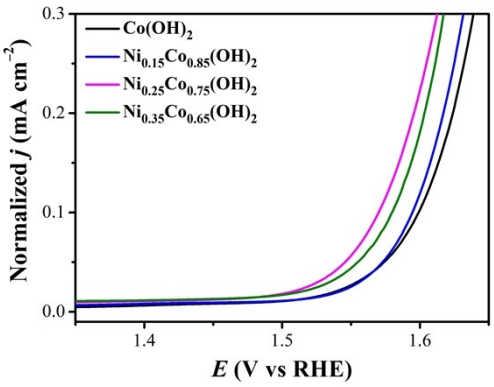

Fig. S11. Normalized LSV curves of the $Co(OH)_2$, $Ni_{0.15}Co_{0.85}(OH)_2$, $Ni_{0.25}Co_{0.75}(OH)_2$, and $Ni_{0.35}Co_{0.65}(OH)_2$.

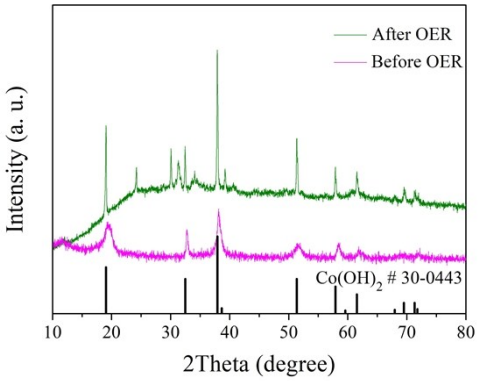

Fig. S12. The XRD pattern of the $Ni_{0.25}Co_{0.75}(OH)_2$ before and after the OER.

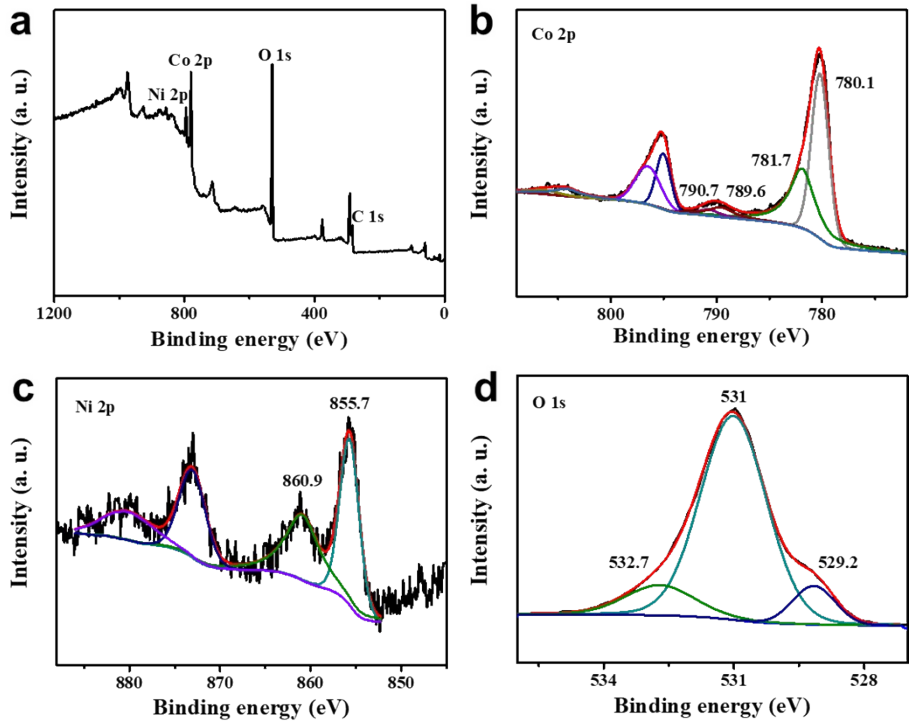

Fig. S13. The XPS full survey (a), high resolution Co 2p (b), Ni 2p (c), and O 1s (d) spectra of the $Ni_{0.25}Co_{0.75}(OH)_2$ after electrocatalysis.